Available online at www.sciencedirect.com
ScienceDirect
Ceramics International 36 (2010) 2493–2498
CERAMICS INTERNATIONAL
www.elsevier.com/locate/ceramint

Short communication

Dehydration reactions and kinetic parameters of gibbsite

Boquan Zhu *, Binxiang Fang, Xiangcheng Li

The State Key Laboratory Breeding Base of Refractories and Ceramics, Wuhan University of Science and Technology, Wuhan 430081, China

Received 18 November 2009; received in revised form 25 March 2010; accepted 18 June 2010
Available online 3 August 2010

Abstract

Dehydration reactions and the corresponding kinetics of gibbsite [γ-$Al(OH)_3$] were analyzed using non-isothermal thermoanalysis and the Kissinger equation. It is concluded that the starting temperature of the dehydration reaction of γ-$Al(OH)_3$ rises with increasing heating rate of the system. At a heating rate of 10 °C min^{-1}, γ-$Al(OH)_3$ has lost part of its crystalline water, and was completely transformed into boehmite (γ-AlOOH)) at about 317 °C. However, γ-AlOOH did not lose the residual crystalline water entirely, and did not change into amorphous Al_2O_3 until the system was above 700 °C. The kinetic energy needed to convert γ-$Al(OH)_3$ to γ-AlOOH, and γ-AlOOH to amorphous Al_2O_3, was calculated by differential scanning calorimetry (DSC) with activation energies of 108.50 and 217.24 kJ mol^{-1}, pre-exponential factors of 2.93×10^9 and 8.30×10^{13}, and reaction orders of 0.96 and 1.06, respectively. The kinetic parameters of dehydration reactions for γ-$Al(OH)_3$ obtained using the derivative thermogravimetric method (DTG) are very similar to that of obtained by DSC.

Keywords: Thermal analysis; Activation energy; Alumina dehydration; Gibbsite dehydration; Kissinger equation

1. Introduction

Various forms of hydrated alumina include trihydrate and monohydrate variants. The trihydrate is divided into gibbsite [γ-$Al(OH)_3$], bayerite (α-$Al(OH)_3$), doyleite and nordstrandite; while the monohydrate form is divided into boehmite (γ-AlOOH)), diaspore (α-AlOOH)) and psendoboehmite [1,2]. The trihydrate form of alumina, especially γ-$Al(OH)_3$, is not only the main raw material source used to produce aluminum oxide by the Bayer method in industry, but is also the hydrated product from calcining ρ-alumina, an important binder used in refractory castables [3–6]. The dehydration temperature, and the corresponding kinetic parameters of γ-$Al(OH)_3$ and its crystalline phase transformation into alumina, have been the focus of research by the ceramics and refractories industries [7–10].

Thermal analysis and X-ray diffraction are usually used to evaluate the phase transitions of alumina. For example, Yang and Yan [11] reported the kinetic study of the phase transformation of γ-alumina to α-alumina using gravimetric analysis measurements at a constant temperature. Wang et al. [12] discussed the kinetic issues when dehydrating γ-$Al(OH)_3$ using X-ray diffraction (XRD). Non-isothermal analysis, such as differential thermal analysis (DTA), differential scanning calorimetry (DSC), and thermogravimetry (TG) are other important methods used to evaluate the phase transformation and the kinetics of inorganic synthesization [13–15]. When compared with isothermal methods, several advantages emerge in the use of non-isothermal techniques, such as simple operation, a broad temperature testing range, and the applicability to reactions with a high rate of phase transformation with temperature [16]. Perić et al. [17] investigated the dehydroxylation of γ-$Al(OH)_3$ into γ-AlOOH by DSC analysis and found the activation energy ranged from 132.92 to 142.26 kJ mol^{-1}. However, the endothermic peak temperature (257–277 °C) of transformation from γ-$Al(OH)_3$ into γ-AlOOH in their research [17] is much lower than the results obtained at the same heating rate (300–320 °C) by other researchers [18,19].

In this study, the dehydration temperature of γ-$Al(OH)_3$ was determined, and its corresponding kinetic parameters were calculated by DSC analysis. Furthermore, derivative thermogravimetric (DTG) analysis was adopted to verify the data determined using DSC analysis. DTG values can be obtained as the first derivative of mass loss to time when the corresponding TG data are measured [20,21].

* Corresponding author. Tel.: +86 27 68862566; fax: +86 27 68862606.
E-mail address: zbqref@263.net (B. Zhu).

0272-8842/$36.00 © 2010 Published by Elsevier Ltd and Techna Group S.r.l.
doi:10.1016/j.ceramint.2010.07.007

In order to simplify the description of the kinetic equations in the paper, all the nomenclature used in them and the corresponding meanings are listed as follows:

A – apparent pre-exponential factor
α_{A^*} – conversion degree reaction extent of reactant A^*
β – heating rate
E – activation energy
$f(\alpha_{A^*})$, $f(w)$ – functions of kinetic model
k – reaction rate constant
n – reaction order
R – universal gas constant (8.314 J mol^{-1} K^{-1})
S – peak shape factor
T – thermodynamic temperature
T_p – peak thermodynamic temperature of DSC curve
t – reaction time
w – residual mass extent of system
w_t, w_0 – residual mass at t time and 0 time of system, respectively

2. Experimental procedure

In order to avoid interference by impurities on the heating effect of γ-Al(OH)$_3$, analytically pure {w[Al(OH)$_3$] > 97.50%, Kermel, Tianjin, China} was utilized in this study. The XRD pattern of this material (Fig. 1) indicated a small amount of γ-AlOOH exists in it (the characteristic diffraction peaks of γ-Al(OH)$_3$ and γ-AlOOH are 0.484505, 0.437383, 0.432421 nm and 0.610700, 0.316050, 0.234460 nm, respectively). The sample was ground into powder with a particle size less than 0.045 mm and a constant mass of 10 ± 0.2 mg used in every test. TG and DSC data were measured simultaneously using a differential scanning calorimeter (Model STA449/6/G, Netzsch, Germany) with a flowing atmosphere of dry argon (50 cm^3 min^{-1}) and a heating rate of 5, 10, 15 and 20 °C min^{-1}, respectively. All test data were processed using the commercial mathematical software, Origin 70 (Origin Lab, USA).

3. Results and discussion

3.1. Dehydration reaction

The TG and DSC curves of sample at the heating rate of 10 °C min^{-1} are shown in Fig. 2. Two major endothermic peaks and one exothermic peak were observed on the DSC curve between 100 and 800 °C. The first endothermic peak begins at 270 °C and ends at 317 °C, with a peak temperature occurring at 300 °C. The second endothermic peak began at 475 °C and ended at 550 °C, with a minimum occurring at 520 °C. The exothermic peak was minor, with a maximum at 725 °C. The TG curve corresponding to endothermic peaks indicates a large mass loss through 317 °C, with other weight changes being minor by comparison.

The degree of γ-Al(OH)$_3$ dehydration with a heating rate of 10 °C min^{-1} at different temperatures is given in Table 1. Up to the end temperature of the first endothermic peak (317 °C), the cumulative mass loss of the sample was 23.87 wt.%, which approached the theoretical mass loss from the conversion of γ-Al(OH)$_3$ to γ-AlOOH (23.08 wt.%). It is concluded that the first endothermic peak (270–317 °C) is induced by the conversion of γ-Al(OH)$_3$ to γ-AlOOH, and the second endothermic peak (475–550 °C) is induced by the conversion from γ-AlOOH to amorphous Al_2O_3, according to the following equations respectively:

$$\gamma\text{-Al(OH)}_3 \rightarrow \gamma\text{-AlOOH} + \text{H}_2\text{O}(23.08\,\text{wt.\%lossintheory}) \quad (1)$$

$$\gamma\text{-AlOOH} \rightarrow 0.5\text{Al}_2\text{O}_3 + 0.5\text{H}_2\text{O}\ (11.54\,\text{wt.\% more loss in theory compared with } \gamma\text{-Al(OH)}_3) \quad (2)$$

It is also observed from Table 1 that the sample still exhibits mass loss during the temperature range from 550–825 °C,

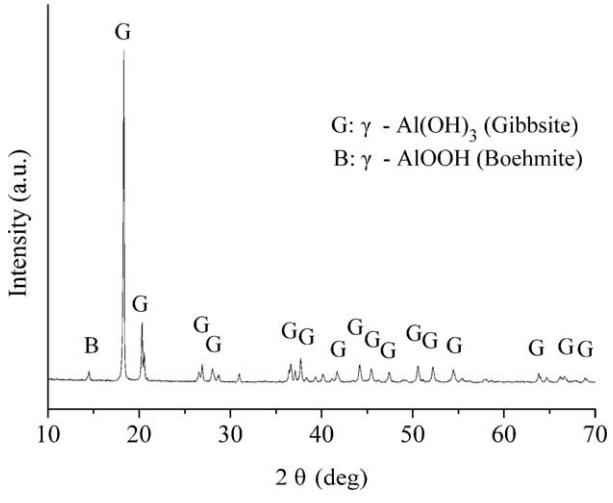

Fig. 1. XRD pattern of a sample high in γ-Al(OH)$_3$ used to study its decomposition.

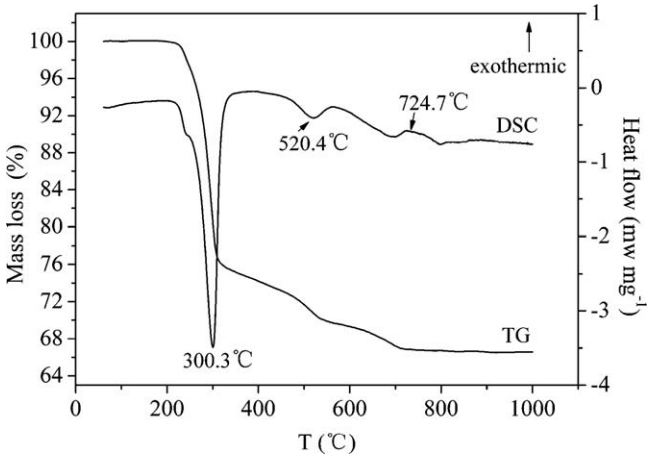

Fig. 2. TG and DSC curves of a test sample heated at 10 °C min^{-1}.

Table 1
Quantitative relationship between temperature and dehydration of γ-$Al(OH)_3$ (heating rate of 10 °C min^{-1}).

	Temperature intervals (°C)							
	<100	100–270	270–317	317–475	475–550	550–650	650–725	725–825
Mass loss (%)	0	5.92	17.95	3.57	2.69	1.38	1.64	0.22
Cumulative mass loss (%)	0	5.92	23.87	27.44	30.13	31.51	33.15	33.37

indicating that the complete dehydration of γ-AlOOH does not terminate at the temperature corresponding to its endothermic peak, but is still occurring at higher temperatures.

3.2. Kinetic parameters of the dehydration reaction

A general heterogeneous reaction is as follows:

$$A^* \rightarrow B_{(s)} + C_{(g)} \quad (3)$$

The reaction rate equation is given by

$$\frac{d\alpha_{A^*}}{dt} = k f(\alpha_{A^*}) \quad (4)$$

or

$$-\frac{dw}{dt} = k f(w) \quad (5)$$

where $f(\alpha_{A^*}) = (1-\alpha_{A^*})^n$ and $f(w) = w^n$, and k is calculated according to the following equation:

$$k = A \exp\left(-\frac{E}{RT}\right) \quad (6)$$

The values of E, A and $f(\alpha_{A^*})$ [or $f(w)$] are the three kinetic factors describing a reaction [22].

Most of the methods that calculate kinetic parameters are derived from Eqs. (4)–(6); among which, the Kissinger method is the one most frequently used in non-isothermal thermo-analysis [23–25]. Dehydration of γ-$Al(OH)_3$ is divided into two stages: the conversion from γ-$Al(OH)_3$ to γ-AlOOH, and the conversion from γ-AlOOH to amorphous Al_2O_3. The Kissinger method was used to calculate kinetic parameters of the two dehydration reactions [γ-$Al(OH)_3$ and γ-AlOOH], respectively.

3.2.1. Determination of kinetic parameters of the first stage by DSC curves

Kissinger made some differential derivation based on Eqs. (4) and (6), deriving the following equation [26]:

$$\ln\left(\frac{\beta}{T_p^2}\right) = \ln\left(\frac{AR}{E}\right) - \frac{E}{R}\frac{1}{T_p} \quad (7)$$

As for different heating rates (β), T_p is also different. A linear plot of $\ln(\beta/T_p^2)$ against $1/T_p$ can be obtained according to Eq. (7). Furthermore, E and A can be calculated from the slope and intercept of the fitted line.

Partial DSC curves of samples at heating rates of 5, 10, 15 and 20 °C min^{-1} showing where the maximum endothermic peak occurs are given in Fig. 3. All beginning, ending, and peak temperatures of each endothermic curve shift to higher temperatures with an increase of heating rate; which means that dehydration temperature of γ-$Al(OH)_3$ is not fixed, but increases with increasing of heating rate. The fitted linear equation between $\ln(\beta/T_p^2)$ and $1000/T_p$ has a high coefficient of correlation ($R^2 = 0.996$), as shown in Fig. 4 [Y and X stand for $\ln(\beta/T_p^2)$ and $1000/T_p$, respectively]; and results in a value of 108.50 kJ mol^{-1} for E, and 2.93×10^9 for A, respectively. The activation energy of conversion from γ-$Al(OH)_3$ to γ-AlOOH

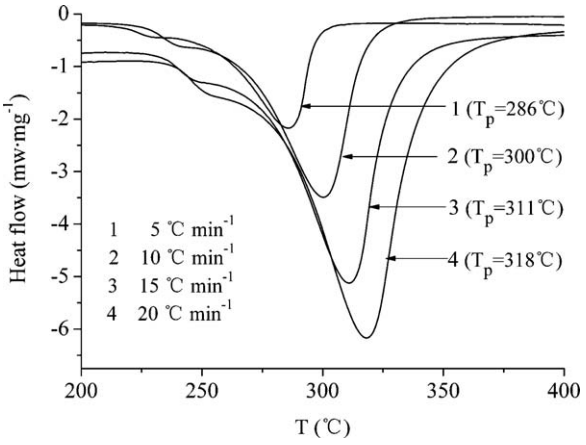

Fig. 3. DSC curves of the same γ-$Al(OH)_3$ starting material at different heating rates during the first dehydration stage.

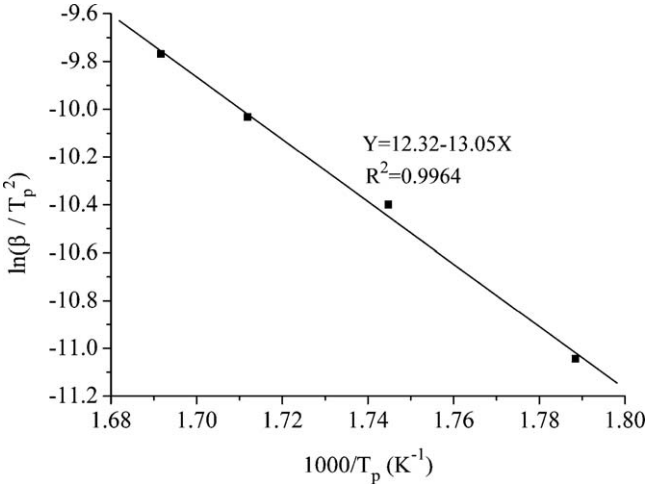

Fig. 4. Plotting $\ln(\beta/T_p^2)$ vs. $1000/T_p$ during the first dehydration stage (between 200 and 400 °C).

obtained in this study is lower compared with the result of Perić et al. [17] (132.92–142.26 kJ mol^{-1}) mainly because of the different decomposition temperature of γ-$Al(OH)_3$.

3.2.2. Determination of kinetic parameters of the first stage by DTG curves

DSC curves indicate the energy changes of γ-$Al(OH)_3$ during dehydration, while TG curves reflect weight changes of the process. Plotting the first derivative of weight loss versus time, i.e. DTG curve, displays more sensitivity to weight changes than temperature by giving greater definition to small weight changes [20,27]. For that reason, DTG curves were used to calculate kinetics parameters of dehydration of γ-$Al(OH)_3$ to verify the accuracy of results derived from DSC curves.

Imitating the differential method of Kissinger, the following equation based on Eqs. (5) and (6) was obtained:

$$\ln\left(-\frac{dw}{dt}\right) = -\frac{E}{RT} + \ln[A f(\alpha)] \tag{8}$$

According to the definition, DTG $= dw/dt$ is the DTG value at time t. Using a group of DTG curves at different heating rates, we can determine the corresponding DTG and T values at certain conversion degrees, fit a line according to different ln(− DTG) and $1/T$ values, then determine E from slope of the fitted line.

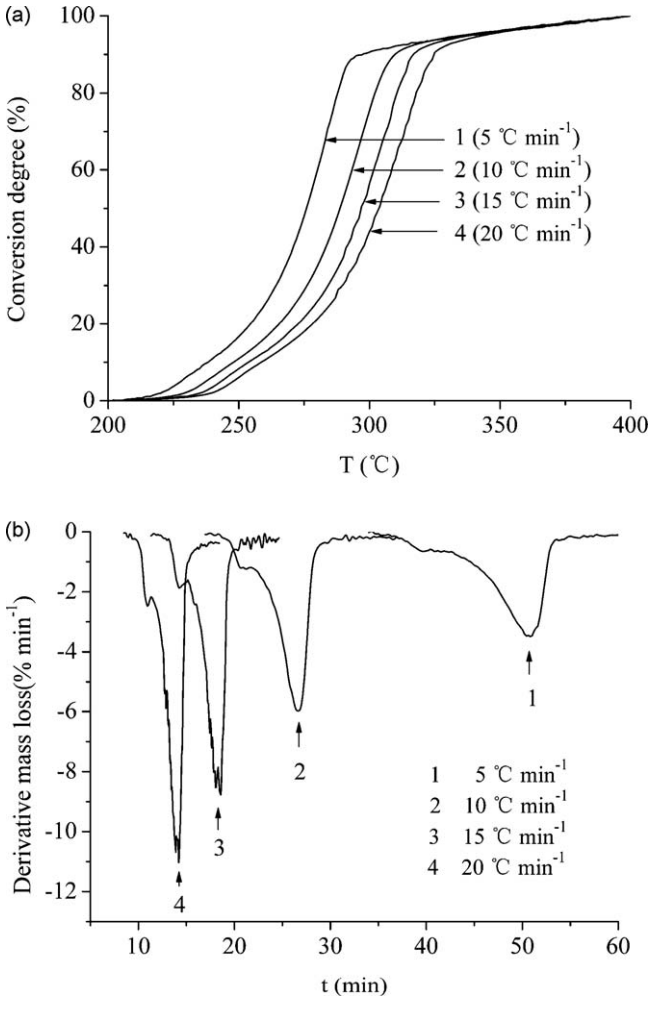

Fig. 5. Conversion degree (a) and DTG (b) curves of sample at different heating rates during the first dehydration stage [γ-$Al(OH)_3$ to γ-AlOOH].

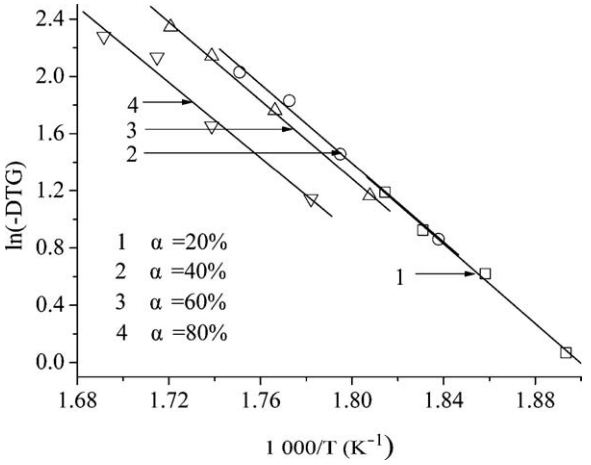

Fig. 6. Fitting lines of ln(− DTG) vs. $1000/T$ at different conversion degree during the first dehydration stage.

The conversion of the first stage [γ-$Al(OH)_3$ to γ-AlOOH] occurs between 200 and 400 °C, so the degree of conversion can be calculated presuming that dehydration starts at 200 °C and ends at 400 °C. According to the temperature corresponding to the given conversion degree (Fig. 5a), the time required to reach the temperature can be determined, and the corresponding DTG value plotted (Fig. 5b). Samples with different heating rates result in different time and different DTG values at the same conversion degree, then a line of ln(− DTG) against $1/T$ can be fitted. In Fig. 6, 4 fitted lines of ln(− DTG) against $1000/T$ at conversion degree of 20, 40%, 60% and 80% are represented respectively as follows:

$$\alpha = 20\%, \quad Y = 26.43 - 13.92X \quad (R^2 = 0.9953) \tag{9}$$

$$\alpha = 40\%, \quad Y = 26.22 - 13.79X \quad (R^2 = 0.9952) \tag{10}$$

$$\alpha = 60\%, \quad Y = 25.90 - 13.68X \quad (R^2 = 0.9983) \tag{11}$$

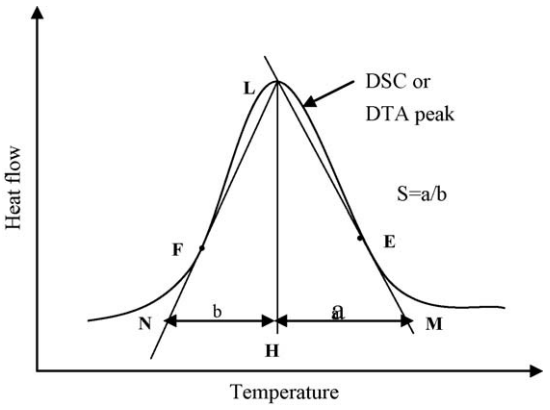

Fig. 7. Diagrammatic sketch of definition for peak shape factor [22].

Table 2
Peak shape factor S and reaction order n of the first stage of γ-$Al(OH)_3$ dehydration.

Heating rate (°C min^{-1})	S	n
5	0.460	0.85
10	0.552	0.94
15	0.627	1.00
20	0.688	1.04

$$\alpha = 80\%, \quad Y = 24.60 - 13.17X \quad (R^2 = 0.9776) \tag{12}$$

where Y is the ln(− DTG) value, X is the 1000/T value, and α is the conversion degree. The slopes of the fitted lines at different conversion degree are similar to each other, and the activation energy E of the first dehydration stage is calculated as 113.40 kJ mol^{-1} based on the average value of the 4 different slopes.

Obviously, the E value calculated from the DTG curves is very close to the one resulting from DSC curves (108.50 kJ mol^{-1}), which means the two methods can be used to calculate the kinetics of γ-$Al(OH)_3$ dehydration.

3.2.3. Reaction order of the first stage

In order to determine the reaction order, n, of the kinetic equation, Kissinger introduced the conception of peak shape factor, S, and defined it as the ratio of a/b shown in Fig. 7 [22]. Details about the values a and b were defined as follows:

For the triangle MNL shown in Fig. 7, the sides ML and NL are tangent lines to a DSC or DTA peak at the right and left inflection points (E and F), respectively. The bottom side MN is a random straight line paralleling to the abscissa, which is divided into 2 line segments MH and NH by the altitude line segment LH. The length of MH is a and the length NH is b.

According to the theoretical derivation of Kissinger, the quantitative relationship between the reaction order (n) and the shape factor (S) is described as follows [22,28]:

$$n = 1.26\,S^{0.5} \tag{13}$$

The peak shape factor, S, and the corresponding n, values of the first dehydration stage of γ-$Al(OH)_3$ at different heating rate were calculated according to Fig. 7 and Eq. (13), respectively. The calculated values for S and n are listed in Table 2. All the reaction order values of the samples at different heating rates are close to 1 except at 5 °C min^{-1}. The average of the 4 reaction order values is 0.96.

3.2.4. Determination of kinetic parameters of the second stage by DSC and DTG curves

The peak temperature, T_p, of the second endothermic peak of γ-$Al(OH)_3$ at heating rates of 5, 10, 15 and 20 °C min^{-1}, is 505, 520, 531 and 535 °C, respectively. Using DSC and DTG data, kinetic parameters of the second dehydration stage of γ-$Al(OH)_3$ were also determined using Eqs. (7), (8) and (13) as 217.24 kJ mol^{-1} for E, 8.30×10^{13} for A, and 1.06 for n.

4. Conclusions

The dehydration of γ-$Al(OH)_3$ is divided into two stages: (1) γ-$Al(OH)_3$ dehydrates partial crystalline water and transforms into γ-AlOOH, and (2) γ-AlOOH dehydrates remaining water and transforms into amorphous Al_2O_3 at higher temperatures. Furthermore, the starting dehydration temperature of γ-$Al(OH)_3$ shifts to higher temperatures as the heating rate of the system increases.

Kinetic parameters, such as: activation energy, the pre-exponential factor, and the reaction order of the two dehydration reactions of γ-$Al(OH)_3$ were calculated using the Kissinger equation, DSC and DTG, respectively. Values produced by DSC and DTG were very similar.

Acknowledgement

Financial support by National Natural Science Foundation of China (No. 50774057) is gratefully acknowledged.

References

[1] M.H. Zhang, Y.Q. Zhang, Research of crystalline phase transformation of alumina by X-ray diffraction at high temperature, Pet. Process. Petrochem. 10 (1979) 56–75.
[2] H.S. Santos, T.W. Campos, P.S. Santos, P.K. Kiyohara, Thermal phase sequences in gibbsite/kaolinite clay: electron microscopy studies, Ceram. Int. 31 (2005) 1077–1084.
[3] B.A. Scott, W.H. Horsman, Structural change during the production of corundum by calculation of gibbsite and their influence on fabrication, Trans. Brit. Ceram. Soc. 69 (1970) 37–43.
[4] R. Salomão, V.C. Pandolfelli, The role of hydraulic binders on magnesia containing refractory castables: Calcium aluminate cement and hydratable alumina, Ceram. Int. 35 (2009) 3117–3124.
[5] F.A. Cardoso, M.D.M. Innocentini, M.F.S. Miranda, F.A.O. Valenzuela, V.C. Pandolfelli, Drying behavior of hydratable alumina-bonded refractory castables, J. Eur. Ceram. Soc. 24 (2004) 797–802.
[6] I.R. Oliveira, V.C. Pandolfelli, Castable matrix, additives and their role on hydraulic binder hydration, Ceram. Int. 35 (2009) 1453–1460.
[7] I. Levin, L.A. Bendersky, D.G. Brandon, M. Rühle, Cubic to monoclinic phase transformations in alumina, Acta Mater. 45 (1997) 3659–3669.
[8] Z.X. Gao, Z.Y. He, X.P. Zheng, Q.H. Fu, X.B. Shi, Phase transformation and morphology of Bayer-gibbsite during heating, J. Chin. Ceram. Soc. 36 (2008) 117–123.
[9] H.S. Yen, J.L. Chang, P.C. Yu, Relationships between DTA and DIL characteristics of nano-sized alumina powders during θ- to α-phase transformation, J. Cryst. Growth 246 (2002) 90–98.
[10] S.D. Vaidya, N.V. Thakkar, Study of phase transformations during hydration of rho alumina by combined loss on ignition and X-ray diffraction technique, J. Phys. Chem. Solids 62 (2001) 977–986.
[11] G.Q. Yang, D.S. Yan, The kinetics of phase transformation of alumina, J. Chin. Ceram. Soc. 5 (1966) 1–11.
[12] H.P. Wang, B.G. Xu, P. Smith, M. Davies, L. Desilva, C. Vingate, Kinetic modelling of gibbsite dehydration/amorphization in the temperature range 823–923 K, J. Phys. Chem. Solids 67 (2006) 2567–2582.
[13] J.P. Elder, Reconciliation of Arrhenius and iso-conversional analysis kinetics parameters of non-isothermal data, Thermochim. Acta 272 (1996) 41–48.
[14] X.D. Li, B.Q. Zhu, Kinetics study of mullite formation from aluminum sulfate and silica in molten sodium sulfate, J. Chin. Ceram. Soc. 36 (2008) 498–502.
[15] N.S. Saxena, Phase transformation kinetics and related thermodynamic and optical properties in chalcogenide glasses, J. Non-Cryst. Solids 345–346 (2004) 161–168.

[16] S. Kurajica, A. Bezjak, E. Tkalčec, Resolution of overlapping peaks and the determination of kinetic parameters for the crystallization of multi-component system from DTA or DSC curves. I. Non-isothermal kinetics, Thermochim. Acta 288 (1996) 123–135.
[17] J. Perić, R. Krstulović, M. Vućak, Investigation of dehydroxylation of gibbsite into boehmite by DSC analysis, J. Therm. Anal. 46 (1996) 1339–1347.
[18] K.J.D. Mackenzie, J. Temuujin, J. Okada, Thermal decomposition of mechanically activated gibbsite, Thermochim. Acta 327 (1999) 103–108.
[19] J.M.R. Mercury, P. Pena, A.H. Aza, On the decomposition of synthetic gibbsite studied by neutron thermodiffractometry, J. Am. Ceram. Soc. 89 (2006) 3728–3733.
[20] J. Yang, R. Miranda, C. Roy, Using the DTG curve fitting method to determine the apparent kinetic parameters of thermal decomposition of polymers, Polym. Degrad. Stab. 73 (2001) 455–461.
[21] A.V. dos Santos, J.R. Matos, Dehydration studies of rare earth *p*-toluenesulfonate hydrates by TG/DTG and DSC, J. Alloys Compd. 344 (2002) 195–198.
[22] R.Z. Hu, Q.Z. Shi, Thermal Analysis Kinetics, Science Press, Beijing, PRC, 2001, pp. 19–22, 111.
[23] A.A. Duswalt, The practice of obtaining kinetic data by differential scanning calorimetry, Thermochim. Acta 8 (1974) 55–68.
[24] S.M. Taylor, P.J. Fryer, A numerical study of the use of the Kissinger analysis of DSC thermograms to obtain reaction kinetic parameters, Thermochim. Acta 209 (1992) 111–125.
[25] I.W. Donald, Crystallization kinetics of a lithium zinc silicate glass studied by DTA and DSC, J. Non-Cryst. Solids 345–346 (2004) 120–126.
[26] H.E. Kissinger, Variation of peak temperature with heating rate in differential thermal analysis, J. Res. Natl. Bur. Stand. 57 (1956) 217–221.
[27] Y.F. Lee, D. Dollimore, The identification of the reaction mechanism in rising temperature kinetic studies based on the shape of the DTG curve, Thermochim. Acta 323 (1998) 75–81.
[28] N.S. Fatemi, R. Whitehead, D. Price, D. Dollimore, Determination of activation energy value from the maximum rate of reaction points obtained from non-isothermal experiments, Thermochim. Acta 78 (1984) 437–440.